The hidden geometry of weighted complex networks

Antoine Allard,[1] M. Ángeles Serrano,[1,2] Guillermo García-Pérez,[1] and Marián Boguñá[1]

[1] *Departament de Física Fonamental, Universitat de Barcelona, Martí i Franquès 1, 08028 Barcelona, Spain*
[2] *Institució Catalana de Recerca i Estudis Avançats (ICREA), Passeig Lluís Companys 23, E-08010 Barcelona, Spain*

(Dated: January 18, 2016)

We present a general and powerful, yet simple, class of weighted networks embedded in hidden metric spaces. This class of weighted networks allows an explicit prescription of the joint degree and strength distributions, and the control of the weight distribution and the local disparity of weights by tuning their coupling with the underlying metric space. We present an approach to estimate whether an underlying metric space is needed to explain the weighted features of real networks and show that the model generates networks that reproduce these properties advantageously. The results suggest that the nontrivial weighted structure of real networks could be explained by the coupling between the weights and an underlying metric space, and open the way to the embedding of real weighted networks and to unveiling their natural hidden geometry.

arXiv:1601.03891v1 [physics.soc-ph] 15 Jan 2016

I. INTRODUCTION

Complex networks [1, 2] have been conjectured to be embedded in hidden metric spaces, in which distances among nodes encode their similarity and, thus, their likelihood of being connected [3]. This hypothesis, combined with a suitable underlying space, has offered a geometric interpretation of the complex topologies observed in real networks, including scale-free degree distributions, the small-world effect, strong clustering as a reflection of the triangle inequality, and self-similarity. It has also explained their efficient inter-node communication without a knowledge of the complete structure [4, 5]. Moreover, it has been shown that for networks whose degree distribution is scale-free, the natural geometry of their underlying metric space is hyperbolic [6–10]. All these results have then been used to propose geometric models for real growing networks that reproduce their evolution and in which preferential attachment emerges from local optimization principles [11, 12]. Finally, mapping real complex networks into a hidden metric space has yielded a sustainable solution to the scaling limitations of the Internet [13], and has shed light on the hierarchical organization of biochemical pathways in cells [14].

These achievements have been accomplished while considering a *binary* network representation in which links either exist or are absent. There exists, however, a class of complex networks for which the magnitude of the interactions between nodes (i.e., the weights) plays a central role in their structural organization and dynamics [15]. For instance, the quantification of the rich-club effect in real weighted networks, in sharp contrast to results in unweighted representations, unveils the formation of alliances in multipolarized environments or the lack of cohesion even in the presence of rich-club ordering [16]. Similarly, the propagation of emergent diseases in the international airports network is intimately linked to the number of passengers flying from one airport to the other [17]. A shift towards a paradigm of weighted networks is therefore in order to fully understand the interplay between their structural organization and their function. While several models have been proposed to address this matter [18–25], none of them, except to some extent the maximum-entropy class of models [26–30], is general enough to reproduce the topology and weighted structure of real weighted complex networks.

In this paper, we present a general and versatile class of weighted networks embedded in hidden metric spaces. Built upon the so-called *Newtonian* class of binary networks in hidden metric spaces [3, 13], our framework preserves all the qualities of complex topologies embedded in underlying metric spaces and, in addition, it allows to enforce explicitly the strength (sum of weights of a node) distribution and the correlation between the strength and the degree of nodes. Moreover, the level of coupling between the weights and the underlying metric space enables to control the local disparity of the weights associated to the nodes [31] as well as the shape of the weight distribution.

Our model lends itself to analytical treatment and includes an approach to estimate whether an underlying metric space is needed to explain the weighted features of real networks. One of the most remarkable aspects of the proposed class of models is the fact that the degree and strength distributions can be adjusted independently of the coupling with the underlying metric space. This critical property opens the path towards the uncovering of the natural geometry or real weighted complex networks. Indeed, using our model, we find strong empirical evidence of metric properties in real networks, not only at the level of their topology but also in their weighted structure.

II. THE MODEL

Our model is a nontrivial generalization to weighted networks of a class of random networks with hidden variables embedded in a metric space [3]. In this model, N nodes are uniformly distributed with density δ in a D-dimensional homogeneous and isotropic metric space [32],

and are assigned a hidden variable κ according to the probability density function (pdf) $\rho(\kappa)$. Two nodes with hidden variables κ and κ' separated by a metric distance d are connected with a probability

$$p(\kappa,\kappa',d)=p(\chi) \quad \text{where} \quad \chi=\frac{d}{(\mu\kappa\kappa')^{1/D}}\ , \tag{1}$$

where $\mu>0$ is a free parameter and $p(\chi)$ is an arbitrary positive function taking values within the interval $(0,1)$. Whenever the integral $\int_0^\infty \chi^{D-1}p(\chi)d\chi$ is bounded, the free parameter μ can be chosen such that $\bar{k}(\kappa)=\kappa$. Hence, κ corresponds to the expected degree of nodes, so the degree distribution can be specified through the pdf $\rho(\kappa)$

$$P(k)=\frac{1}{k!}\int \mathrm{e}^{-\kappa}\kappa^k\rho(\kappa)d\kappa\ , \tag{2}$$

regardless of the specific form of $p(\chi)$ (see Apps. A 1 and A 2 for details). The freedom in the choice of $p(\kappa,\kappa',d)$ allows us to tune the level of coupling between the topology of the networks and the metric space, which in turn allows us to control many properties such as the clustering coefficient and the navigability [3, 5]. Moreover, the form of the connection probability in Eq. (1) implies that networks generated with this model are small worlds for any heterogeneous pdf $\rho(\kappa)$ since high degree nodes are then likely to be connected regardless of the metric distance between them [3, 4].

To generalize this model to weighted networks, a second hidden variable σ is associated to each node. This new hidden variable can be correlated with κ so, hereafter, we assume that the pair of hidden variables (κ,σ) associated with the same node are drawn from the joint pdf $\rho(\kappa,\sigma)$. The weight of an *existing* link between two nodes with hidden variables κ, σ, κ' and σ', respectively, and at a metric distance d is distributed according to the pdf

$$\phi(w|\kappa,\sigma,\kappa',\sigma',d)=\frac{1}{\bar{w}}f\left(\frac{w}{\bar{w}}\right)\ , \tag{3}$$

where $f(\epsilon)$ is any probability density function in the domain $[0,\infty)$ with $\langle\epsilon\rangle=1$, and where

$$\bar{w}=\frac{\nu\sigma\sigma'}{(\kappa\kappa')^{1-\alpha/D}d^\alpha}\ , \tag{4}$$

with $\nu>0$ and $0\leq\alpha<D$. The particular form of the distribution of weights Eq. (3) implies that the weight between nodes i and j can be written as

$$\omega_{ij}=\epsilon_{ij}\frac{\nu\sigma_i\sigma_j}{(\kappa_i\kappa_j)^{1-\alpha/D}d_{ij}^\alpha} \tag{5}$$

where ϵ_{ij} is a random variable drawn from the pdf function $f(\cdot)$. Equations (3) and (4) constitute the keystone of our model. Indeed, as shown in App. A 3, the form of Eq. (4) is the only ensuring that $\bar{s}(\sigma)=\sigma$, provided that the integral $\int_0^\infty \chi^{D-\alpha-1}p(\chi)d\chi$ converges. The new hidden variable σ can therefore be interpreted as the expected strength of a node, and the joint pdf $\rho(\kappa,\sigma)=\rho(\kappa)\rho(\sigma|\kappa)$ controls the correlation between degrees and strengths in the network. Indeed, as shown in App. A 4, the average strength of nodes with a given degree, $\bar{s}(k)$, relates to the first moment of the conditional pdf $\rho(\sigma|\kappa)$, $\bar{\sigma}(\kappa)$, through the relation

$$\bar{s}(k)=\frac{1}{(k-1)!P(k)}\int \mathrm{e}^{-\kappa}\kappa^{k-1}\rho(\kappa)\bar{\sigma}(\kappa)d\kappa. \tag{6}$$

Therefore, when $\lim_{\kappa\to\infty}\bar{\sigma}(\kappa)=\infty$ then $\bar{s}(k)\sim\bar{\sigma}(\kappa)$. This limit stands as a good approximation for the behaviour of high degree nodes in real weighted networks.

Remarkably, these relations hold independently of the specific form of the connection probability $p(\chi)$ and of the distribution of weights $f(\epsilon)$, thus conferring great versatility to our model. Even more remarkable, the shape of the connection probability $p(\chi)$ and the value of the parameter α—coupling topology and weights to the metric space—do not affect the relations $\bar{k}(\kappa)=\kappa$ and $\bar{s}(\sigma)=\sigma$ and, therefore, the join degree-strength distribution $P(k,s)$. This property conveys a degree of control over the weight distribution as well as over the disparity of nodes which is independent of the specification of degrees and strengths and, more importantly, opens the possibility to measure the metric properties of complex weighted networks.

A. The weighted $\mathbb{S}^1$ model, $\mathbb{WS}^1$

All results presented in the previous section hold in arbitrary dimension and for any form of the connection probability $p(\chi)$ and weight probability density $f(\epsilon)$ in Eqs. (1) and (3). To apply the formalism to real weighted networks, we particularize to the $\mathbb{S}^1$ model as generator of the topology [3]. In that model, we choose the circle $\mathbb{S}^1$ of radius $R=N/2\pi$ to be the underlying geometry over which nodes are uniformly distributed with density $\delta=1$. Distances among nodes are measured in terms of arc lengths, that is, two nodes with angular positions θ and θ' are therefore at a distance $d(\theta,\theta')=R\Delta\theta$ where $\Delta\theta=\pi-|\pi-|\theta-\theta'||$. The connection probability is set to

$$p(\chi)=\frac{1}{1+\chi^\beta} \quad \text{with} \quad \chi=\frac{d}{\mu\kappa\kappa'}, \tag{7}$$

where $\beta>1$ is a free parameter that can be used to tune the clustering. Equation (7) casts the ensemble of networks generated by the model into exponential random networks [6], i.e., networks that are maximally random given the constraints imposed by the free parameters (that is, $\rho(\kappa)$ and β). To obtain a scale-free degree distribution, hidden variables κ are distributed according to

$$\rho(\kappa)=\frac{(\gamma-1)\kappa_0^{\gamma-1}\kappa^{-\gamma}}{1-(\kappa_c/\kappa_0)^{1-\gamma}} \tag{8}$$

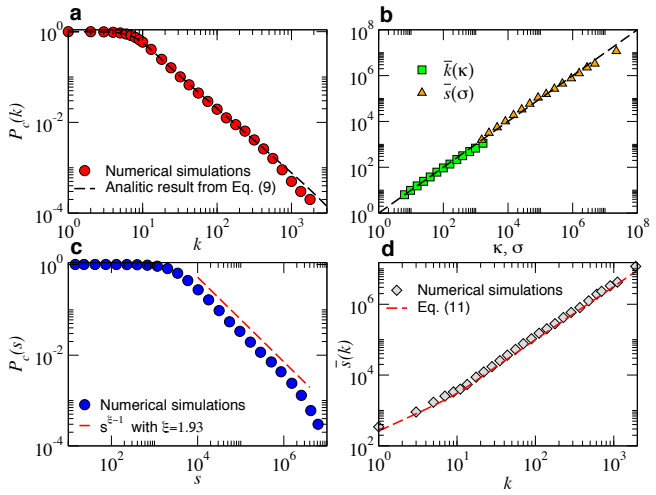

FIG. 1. Properties of the model and validation of the theoretical calculations given in Sec. II A. Numerical simulations correspond to a single network of size $N = 10^4$ and parameters $\alpha = 0.4$, $\beta = 1.5$, $\gamma = 2.4$, $\eta = 1.5$, $\langle k\rangle = 20$, $\kappa_c = \kappa_0 N^{1/(\gamma-1)}$, $a = 100$, and noise $\langle \epsilon^2\rangle = 1.5$. **a**, complementary cumulative degree distribution compared with the prediction given by Eq. (10). **b**, average degree and average strength of nodes as a function of their hidden variables κ and σ. The deviation for high κ and σ is due to the finite size of the network and disappears as $N \to \infty$. **c**, complementary cumulative strength distribution. The dashed line indicates a scaling $\propto s^{-\xi}$ with $\xi = (\gamma+\eta-1)/\eta \simeq 1.93$, as expected. **d**, average strength as a function of degree. The dashed line shows the prediction of Eq. (12).

with $\kappa_0 < \kappa < \kappa_c$ and $\gamma > 1$. Notice that by keeping the explicit dependence in the upper cutoff it is possible to model networks with $\gamma < 2$ and a hard cutoff, as found for instance in airport networks [15]. Moreover, since it is generally more convenient to fix the average degree $\langle k\rangle$ explicitly, we choose κ_0 such that

$$\langle \kappa\rangle = \int_{\kappa_0}^{\kappa_c} \kappa\rho(\kappa)d\kappa = \frac{(\gamma-1)\kappa_0}{(\gamma-2)}\frac{1-(\kappa_c/\kappa_0)^{2-\gamma}}{1-(\kappa_c/\kappa_0)^{1-\gamma}} = \langle k\rangle \ , \tag{9}$$

and fix the remaining free parameters κ_c and γ externally [33]. From Eq. (2), we expect

$$P(k) = \frac{(\gamma-1)\kappa_0^{\gamma-1}}{1-(\kappa_c/\kappa_0)^{1-\gamma}}\frac{\Gamma(k-\gamma+1,\kappa_0,\kappa_c)}{k!} \sim \frac{(\gamma-1)\kappa_0^{\gamma-1}k^{-\gamma}}{1-(\kappa_c/\kappa_0)^{1-\gamma}} \ , \tag{10}$$

where $\Gamma(x,\kappa_0,\kappa_c)$ is the generalized incomplete gamma function [34].

To assign weights on top of the topology generated by the model, the noise distribution in Eq. (3) is chosen to be a gamma distribution of average $\langle\epsilon\rangle = 1$, that is,

$$f(\epsilon) = \frac{\lambda^\lambda}{\Gamma(\lambda)}\epsilon^{\lambda-1}e^{-\lambda\epsilon} \ \text{ with } \ \langle\epsilon^2\rangle = 1+\frac{1}{\lambda}. \tag{11}$$

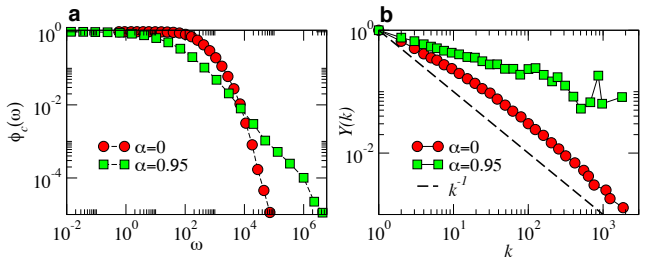

FIG. 2. Effect of the underlying geometry. Simulations correspond to synthetic networks with the same parameters as in Fig. 1 but with two different values of the coupling parameter α. **a**, complementary cumulative weight distribution for $\alpha = 0$ (no coupling with the hidden metric space) and $\alpha = 0.95$ (strong coupling). **b**, average disparity of nodes as a function of their degree for the same values of the coupling α. The dashed line shows the scaling k^{-1}, corresponding to the a perfect equipartition of the strength of a node among its links.

This particular choice allows us to interpolate with a single parameter between a zero noise limit when $\lambda \gg 1$, exponential noise when $\lambda = 1$, and strongly heterogeneous noise when $\lambda \ll 1$. Finally, to control the correlation between strength and degree and, therefore, to tune the strength distribution, we assume a deterministic relation between hidden variables σ and κ of the form $\sigma = a\kappa^\eta$, as observed in real complex networks [15]. From Eq. (6), we thus expect

$$\bar{s}(k) = \frac{ak\Gamma(k-\gamma+\eta,\kappa_0,\kappa_c)}{\Gamma(k-\gamma+1,\kappa_0,\kappa_c)} \sim ak^\eta \ . \tag{12}$$

Notice that the relation between average strength and degree in the previous expression is totally independent of the underlying metric space. It implies that the strength distribution scales as $P(s) \sim s^{-\xi}$ for $s \gg 1$ with $\xi = (\gamma+\eta-1)/\eta$. Figure 1 shows the basic topological and weighted properties of a network generated using Eqs. (7)–(12) and compares them to the theoretical predictions presented in this section. Apart from some expected fluctuations due to finite size, the agreement between the two is excellent.

B. The effect of the underlying geometry

Geometry has a strong effect on the strength and weight distributions, which depend on the coupling parameter α. In fact, as shown in Appendix A, the second moment of the strength distribution $\langle s^2\rangle$ is proportional to the integral $\int_0^\infty \chi^{-2\alpha}p(\chi)d\chi$, which diverges whenever $\alpha > 1/2$. The origin of these fluctuations is rooted in the strong constraints that geometry imposes on the weights of individual links. In the absence of coupling (i.e., $\alpha = 0.0$) the metric distance between nodes does not influence the magnitudes of the weights. Consequently, the distribution of weights generated by the model is the

original pdf in Eqs. (3) and (4) convoluted with the distribution of values of the ratio $\sigma\sigma'/\kappa\kappa'$. Conversely, in the case of strong coupling (i.e., $\alpha \lesssim 1$), short range links are constrained to have larger weights whereas long range ones have small weights. This effect increases the heterogeneity in the weight distribution and causes the divergence of $\langle s^2 \rangle$ when $\alpha > 1/2$. Figure **2a** shows this effect on synthetic networks generated with the model with identical parameters except for the value of α.

The same effect is visible in the local heterogeneity of the weights attached to a given node. To characterize such heterogeneity, we use the disparity measure defined as

$$Y_i = \sum_j \left(\frac{w_{ij}}{s_i} \right)^2 , \tag{13}$$

where w_{ij} is the weight of the link between nodes i and j ($w_{ij} = 0$ if there is no link) and $s_i = \sum_j w_{ij}$ [31]. In Fig. **2b**, we see that in the absence of coupling (i.e., $\alpha = 0.0$) the disparity scales as $Y_i \sim k_i^{-1}$ corresponding to the situation in which weights are roughly homogeneously distributed among the links [35]. On the other side of the spectrum, we see that under maximal coupling (i.e., $\alpha \lesssim 1$), the disparity decreases slower than k_i^{-1} meaning that weights are heterogeneous and that the large strength of nodes is due to a handful of links with large weights.

III. HIDDEN METRIC SPACES UNDERLYING REAL WEIGHTED NETWORKS

As already discussed, our class of models has the critical ability to fix the local properties of the network, namely the joint degree-strength distribution, while changing the level of coupling with the metric space, quantified by parameter α. This allows us to discern whether a metric space is needed to explain the observed topological and weighted properties of real complex networks and to compare them with synthetic networks generated with the model.

A. Measuring the triangle inequality in hyperbolic space $\mathbb{WH}^2$

Given a real weighted complex network, how can we determine whether its weighted organization is influenced by any means by the properties of an underlying metric space? An answer to this question must necessarily go through a test of the triangle inequality. The triangle inequality is one of the fundamental properties of any metric space. In simple words, it states that whenever point A is close to point B and point B is close to point C, then points A and C must also be close. In the case of networks embedded in metric spaces, the triangle inequality induces the existence of a large number of triangles in the graph and so a high clustering coefficient that remains finite even for model networks in the thermodynamic limit. Considering the topology of the network without an explicit embedding of the network, a direct check of the triangle inequality is not possible as the binary structure of the graph does not contain information about distances between nodes. An indirect empirical evidence of the connection between complex networks and hidden metric spaces can nevertheless be found by analyzing the self-similarity properties of the degree-dependent clustering coefficient [3].

In contrast, weights associated to connections among nodes in weighted networks do contain information about their distances in the metric space so that, in principle, a direct check of the triangle inequality should be possible. In order to ensure that the metric properties of triples in the graph are in correspondence to the metric properties of the corresponding triangles in the underlying space, only triples of nodes forming triangles in the graph are taken into account to evaluate the triangle inequality. There are however two main problems when one tries to apply this program. The first problem is related to the fact that connections in the $\mathbb{WS}^1$ model depend not only on angular distances but also on hidden degrees such that we need first a purely geometrical formulation of the weighted hidden metric space network model. The second issue is related to the intrinsic noise present in the system due to the stochastic nature of the processes conforming it. Below, we propose a way to overcome these two limitations.

Notice that, as shown in [6], the model described by Eq. (1) is equivalent, in the one dimensional case, to a purely geometric model where nodes are embedded within a disk of radius R in the hyperbolic plane of constant curvature -1. Indeed, by mapping the hidden variable κ to a radial coordinate r as follows

$$r = R - 2\ln\left[\frac{\kappa}{\kappa_0}\right] \quad \text{with} \quad R = 2\ln\left[\frac{N}{\mu\pi\kappa_0^2}\right] \tag{14}$$

and keeping the same angular coordinates, the connection probability Eq. (1) can be written as

$$p\left(\frac{d}{\mu\kappa\kappa'}\right) = p\left(e^{\frac{1}{2}(x-R)}\right) \tag{15}$$

where $x = r + r' + 2\ln\frac{\Delta\theta}{2}$ is a very good approximation of the hyperbolic distance between two points at radial coordinates r and r' and angular separation $\Delta\theta$. Under this framework, graphs generated with our model are geometric random graphs in the hyperbolic plane and, consequently, the triangle inequality must hold in hyperbolic geometry. To check the triangle inequality, we can then select as triples of points the vertices of topological triangles in the graph, with the condition that distances between these nodes are the hyperbolic ones.

By using the mapping Eq. (14), the weight between nodes i and j in Eq. (5) transforms into

$$\omega_{ij} = \epsilon_{ij} \frac{\nu}{\mu^\alpha} \frac{\sigma_i\sigma_j}{\kappa_i\kappa_j} e^{-\frac{\alpha}{2}(x_{ij}-R)}, \tag{16}$$

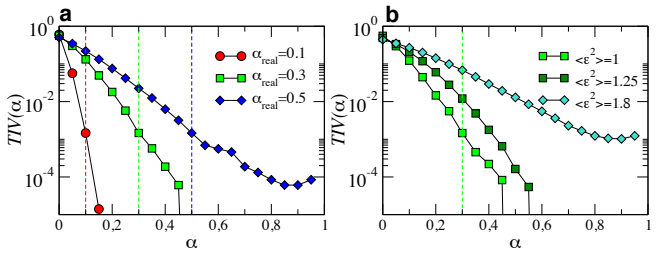

FIG. 3. Triangle inequality violation $TIV(\alpha)$. **a**, without noise and different values of α and **b**, with a fixed value of $\alpha = 0.3$ and different values of the noise $\langle\epsilon^2\rangle$. In both cases, the topology is the same, with $\gamma = 2.5$, $\beta = 2$, $\eta = 1$, and $N = 10^4$. The vertical dashed lines indicate the values of α_{real} used to generate each network.

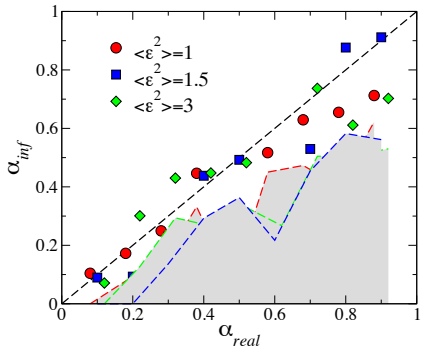

FIG. 4. α_{inf} vs. α_{real} for synthetic networks generated with the model for different values of noise $\langle\epsilon^2\rangle$. In all cases, network topologies are generate with $\gamma = 2.5$, $\beta = 2$, $\eta = 1.2$, $\langle k\rangle = 10$, and $N = 10^4$. The solid gray area indicates the lower bounds found by the method.

from where it is possible to get an estimate of the hyperbolic distance x_{ij} between the two nodes. By using this method, the triangle inequality $x_{ij} + x_{jk} \geq x_{ik}$ becomes

$$\ln\left[\frac{\omega_{ij}\omega_{jk}}{\omega_{ik}}\left(\frac{\kappa_j}{\sigma_j}\right)^2\right] + \ln\left[\frac{\mu^\alpha}{\nu}\right] - \frac{1}{2}\alpha R \leq \ln\left[\frac{\epsilon_{ij}\epsilon_{jk}}{\epsilon_{ik}}\right]. \tag{17}$$

The first term in the left hand side of this inequality is a function of the actual weights and network topology and, thus, can be empirically measured in any network. The next two terms on the left hand side have an explicit dependence on the parameter α [36], which tunes the coupling between the intensity of weights and the underlying metric space. The term in the right hand side is a noise term whose mean value is close to zero.

Let us first assume that this noise term is zero. In this case, the inequality should hold approximately for any value of α equal to or larger than the value of α_{real} used to generate the graph. The inequality does not hold exactly because some of the triangles in the graph may have been generated by chance and, thus, they are unrelated to the metric distances among their vertices. We then propose to measure, for a fixed topology and different values of α, the triangle inequality violation spectrum $TIV(\alpha)$ defined as the ratio between the number of times the triangle inequality is violated (left hand side of Eq. (17) is positive) and the number of triangles in the graph. In the absence of noise, $TIV(\alpha)$ should take a very small value when $\alpha \geq \alpha_{real}$ if the weighted structure of the network is congruent with the existence of an underlying metric space. In Fig. 3**a**, we show $TIV(\alpha)$ for synthetic networks generated with the model with different values of α. As predicted, the curves fall rapidly precisely at the real values of α, as indicated by the dashed vertical lines.

In real situations, however, noise is typically present and has an impact on function $TIV(\alpha)$. Indeed, Fig. 3**b** shows its behavior for a fixed value of α and different values of the noise $\langle\epsilon^2\rangle$. This implies that, to obtain the value of α_{real} from the spectrum $TIV(\alpha)$, we need an independent measure of the noise. For this purpose, we use the square of the coefficient of variation of the strength evaluated in Appendix A, which reads

$$CV^2(s) = \frac{\langle s^2\rangle}{\langle s\rangle^2} - 1 = \frac{\langle\sigma^2/\kappa\rangle^2 I_5}{2\mu\langle\sigma\rangle^4 I_3^2}\langle\epsilon^2\rangle. \tag{18}$$

The left hand side in this equation can be directly measured from the network. The right hand side depends linearly on the noise $\langle\epsilon^2\rangle$ whereas its pre-factor depends both on the topology and on α_{real} through the integrals I_3 and I_5 (see Appendix A for technical details). With all these results at hand, we can define a procedure to test the triangle inequality in any real complex network and, from it, to infer the value of α_{real} that best matches the empirical observations. The test is fully described in Appendix B. Very briefly, we estimate the values of parameter α and $\langle\epsilon^2\rangle$ which best reproduce simultaneously the coefficient of variation of the strength in Eq. (18) and the spectrum $TIV(\alpha)$ of the real network. In Fig. 4, we show the result of this program in the case of synthetic networks with different values of α_{real} and of noise levels. As it can be seen, the inferred values of α match the true values in most of the cases. Our method also allows us to find lower bounds on the inferred values, as shown by the gray areas in Fig. 4. The most remarkable aspect of the test is that it can be performed without any explicit embedding of the network and, thus, it can be readily applied to real networks for which an embedding is not available. In the next section, we analyze three different real weighted complex networks and show that not only the topology can be nicely reproduced by our model but also that the architecture of weights can be fully explained by the existence of a metric space.

B. Comparison with real networks

Next, we study three real-world weighted complex networks from different domains: version iJO1366 of the metabolic network of the bacteria *Escherichia coli*

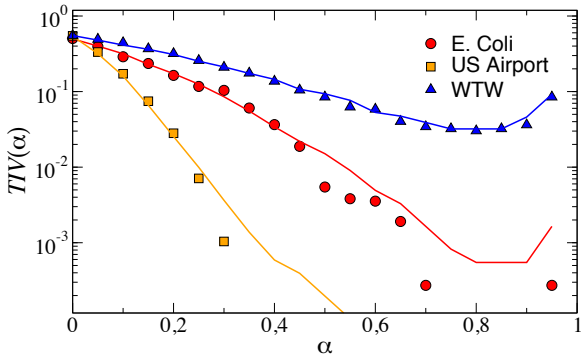

FIG. 5. Triangle inequality violation curves for the three real networks considered (symbols). Solid lines correspond to their model counterparts with the model parameters in Table I.

TABLE I. Model parameters used to reproduce real networks. Note that the value of N is not the measured value in the real network because the model generates nodes with zero degree. Similarly, the value of $\langle k \rangle$ is higher than the measured one to account for finite size effects. With these parameters, generated synthetic networks end up having the same number of non-zero degree nodes and average degree.

	α	β	γ	η	$\langle k \rangle$	κ_c	a	$\langle \epsilon^2 \rangle$	N
E. Coli iJO1366	0.45	2.0	2.5	1.1	7.25	249	1.1	1.3	1100
US Airports 2013	0.15	1.65	1.6	1.7	10.6	500	11900	1.4	1175
WTW 2013	0.41	2.5	2.4	1.6	7.7	800	3800	1.3	189

(E. coli) K-12 MG1655 [37], the US airport network in 2013 [38], and the world trade web (WTW) [39]. We reconstruct a metabolic network representation in which two metabolites are connected by a weighted link accounting for the number of different metabolic reactions in which both participate. In the US airport network, two airports are connected by a weighted link measuring the total number of passengers traveling between them during the year 2013. Finally, weights in the WTW measure the total trade between pairs of countries in the world during the year 2013. Due to their high average degree, the US airport network and the WTW are filtered by the disparity filter defined in [40] to preserve the most statistically significant interactions. In the US airport network, the filtered network coincides with the network defined by regular commercial flights. In the WTW, the filter is able to recover the correlation between degrees of countries and economic indicators, in particular their gross domestic products [41].

We applied the method described in Appendix B to infer α and $\langle \epsilon^2 \rangle$ for the three real networks finding strong evidence of metric properties, both at the topological and weighted levels. Indeed, in Fig. 5, we show the triangle inequality violation curves for the three real networks studied and the same curves for synthetic networks gen-

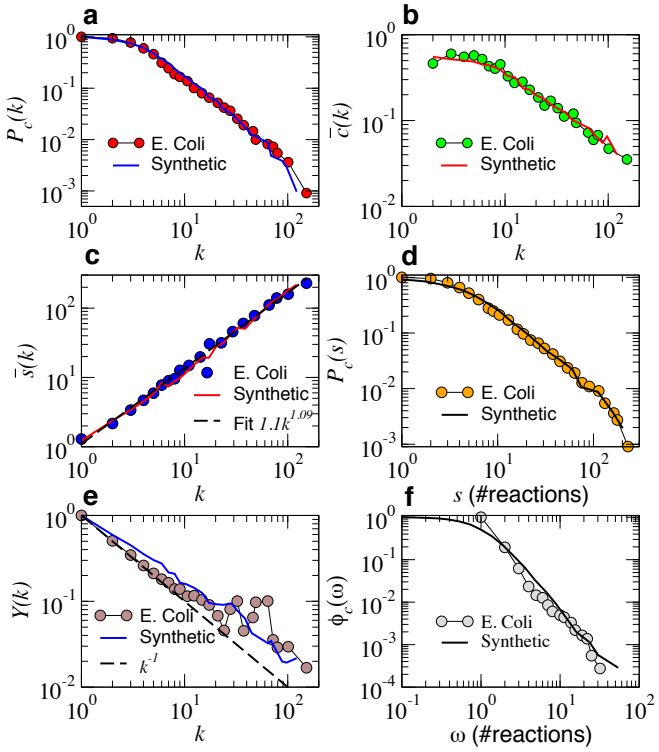

FIG. 6. Comparison between topological and weighted properties of the iJO1366 *E. coli* metabolic network (symbols) and a synthetic network generated by the model with the parameters given in Table I (solid lines). **a**, complementary cumulative degree distribution. **b**, degree-dependent clustering coefficient. **c**, average strength of nodes of degree k. **d**, complementary cumulative strength distribution. **e**, disparity of nodes as a function of their degree. **f**, complementary cumulative weight distribution of links.

erated by the model with values of the coupling parameter α and noise level $\langle \epsilon^2 \rangle$ inferred by our method from the real data. In the three cases, the agreement is excellent, suggesting that the coupling with a metric space is a most plausible explanation of the observed weighted architecture. In Table I, we show the optimal parameters for the three networks. Using these parameters, we generate synthetic networks and confront their topological and weighted properties against the *E. coli* metabolic network in Fig. 6. The agreement between the model and the real network is excellent in all measured properties. The analyses of the US airport network and the WTW is shown in Fig. 7 and Fig. 8, respectively.

IV. DISCUSSION

In this work, we have presented a new class of weighted networks embedded in (hidden) metric spaces. This versatile class of networks explicitly prescribes the degree and strength distributions, as well as the correlation between them, independently of the coupling with the met-

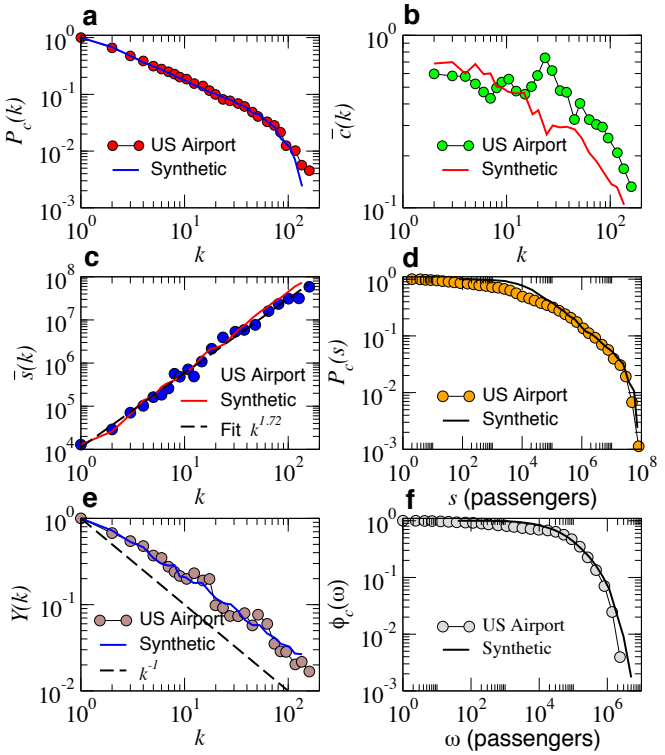

FIG. 7. Comparison between topological and weighted properties of the US airport network and a synthetic network generated by the model with the parameters given in Table I. **a**, complementary cumulative degree distribution. **b**, degree-dependent clustering coefficient. **c**, average strength of nodes of degree k. **d**, complementary cumulative strength distribution. **e**, disparity of nodes as a function of their degree. **f**, complementary cumulative weight distribution of links.

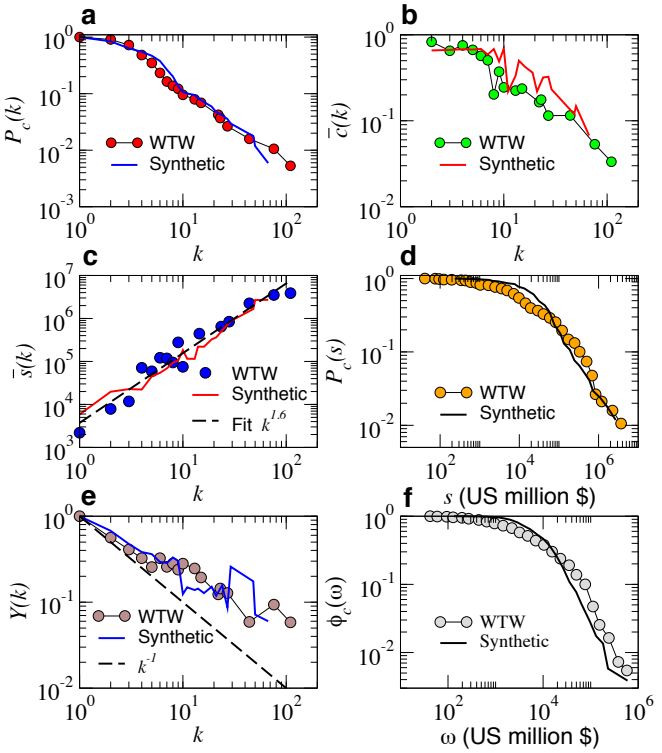

FIG. 8. Comparison between topological and weighted properties of the WTW and a synthetic network generated by the model with the parameters given in Table I. **a**, complementary cumulative degree distribution. **b**, degree-dependent clustering coefficient. **c**, average strength of nodes of degree k. **d**, complementary cumulative strength distribution. **e**, disparity of nodes as a function of their degree. **f**, complementary cumulative weight distribution of links.

ric space. This allows us to reproduce the supra-linear relationship between strength and degree observed in real weighted complex networks and, at the same time, other relevant properties such as the weight distribution, disparity measure, and triangle inequality, which are strongly affected by the coupling with the metric space. The assessment of the triangle inequality allowed us to find strong empirical evidence of metric properties in the weighted architecture of three real complex networks from very different domains. Two of them—the US airport network and WTW—are naturally embedded on the surface of the Earth and, therefore, it would not be totally surprising to find a metric dependence at the weighted level. It is however important to notice that the distance in our model is not the geodesic distance on the Earth but an effective (hyperbolic) distance encoding all the particularities of the system. In any case, the test of the triangle inequality that we have devised does not make use of any explicit embedding but only of the network topology and the corresponding weights and, consequently, can be applied to any weighted network. In particular, the iJO1366 metabolic network of the bacteria *E. coli* is not embedded in any obvious metric space. The high value of α inferred by our method for this network, together with the high levels of clustering and the quality of the previous embedding of its topology [14], provides yet another empirical evidence towards the existence of hidden metric spaces shaping the architecture of this system and, more generally, of real complex networks [3].

The class of binary networks embedded in hidden metric spaces that our new model builds upon has a purely geometrical equivalent whose natural geometry is hyperbolic [6, 42]. Using this class of models, it has been possible to map real complex networks into the hyperbolic plane with an excellent congruency [13, 40, 41]. In the case of the Internet, for instance, such mapping offers a sustainable and realistic solution to the scaling limitations of the Internet routing architecture. Similarly, the work presented in this paper paves the way towards the unveiling of the natural geometry of weighted complex networks. This will lead to a deeper understanding of their structural organization, which will in turn offer insights on their dynamics and on the impact they have on the dynamical processes they support.

ACKNOWLEDGMENTS

We acknowledge support from the James S. McDonnell Foundation Scholar Award in Complex Systems; the Fonds de recherche du Québec – Nature et technologies; the ICREA Academia prize, funded by the Generalitat de Catalunya; the MINECO project no.FIS2013-47282-C2-1-P; the Generalitat de Catalunya grant no.2014SGR608; and APVV (project APVV-0760-11).

Appendix A: Theoretical calculations in a D-dimensional metric space

Most of the theoretical calculations for the model presented in Sec. II are carried out using the probability density function (pdf) $g(k,s|\kappa,\sigma)$ corresponding to the probability that a node with hidden variables κ and σ has a degree equal to k and a strength in the interval $[s,s+ds)$. To compute this pdf, we first consider a pair of nodes whose positions in space are $\boldsymbol{x_i}$ and $\boldsymbol{x_j}$ and whose hidden variables are κ_i, σ_i and κ_j, σ_j, respectively. The pdf for the weight w_{ij} between these two nodes ($w_{ij}=0$ means that there is no link) is

$$\Phi(w_{ij}|\kappa_i,\sigma_i;\kappa_j,\sigma_j;d_{ij}) = [1-p(\kappa_i,\kappa_j,d_{ij})]\delta(w_{ij}) + p(\kappa_i,\kappa_j,d_{ij})\phi(w_{ij}|\kappa_i,\sigma_i,\kappa_j,\sigma_j,d_{ij})\Theta(w_{ij}) \ , \tag{A1}$$

where $\delta(\cdot)$ is the Dirac delta function and $\Theta(\cdot)$ is the left-continuous Heaviside step function (i.e., $\Theta(0)=0$). Without loss of generality, we take the perspective of node i, place it at the origin of the coordinate system, and integrate over the possible values of the hidden variables of node j

$$\Phi(w_{ij}|\kappa_i,\sigma_i) = \iiint \frac{\rho(\kappa_j,\sigma_j)}{V_D}\Phi(w_{ij}|\kappa_i,\sigma_i;\kappa_j,\sigma_j;d_{ij})d\boldsymbol{x_j}d\sigma_j d\kappa_j \ . \tag{A2}$$

In this last equation, $1/V_D$ is the (uniform) pdf for the position of nodes in the metric space. This last expression does not depend on the position of node i due to the isotropy, homogeneity and large size ($N\gg 1$) of the metric space. Because the weights $\{w_{ij}\}_{i,j=1,\ldots,N}$ are assigned independently in the model, the probability that a node has a degree k_i and a strength s_i is equal to the product of the contribution of each potential $N-1$ links, given that the number of existing links is equal to k_i and that their weights sum up to s_i

$$g(k_i,s_i|\kappa_i,\sigma_i) = \prod_j \left[\int \Phi(w_{ij}|\kappa_i,\sigma_i)dw_{ij}\right]\delta\left(k_i-\sum_l \Theta(w_{il})\right)\delta\left(s_i-\sum_l w_{il}\right) \ . \tag{A3}$$

Although it is not possible to further the calculation and obtain a closed form the the pdf $g(k,s|\kappa,\sigma)$, many useful results can be obtained using its generating function defined as

$$\hat{g}(x,y|\kappa_i,\sigma_i) = \sum_{k_i=0}^{N-1}\int_0^\infty g(k_i,s_i|\kappa_i,\sigma_i)x^{k_i}\mathrm{e}^{-s_i y}ds_i \ , \tag{A4}$$

which, dropping the subscripts i and j, can be written as

$$\hat{g}(x,y|\kappa,\sigma) = \left[\iiint \frac{\rho(\kappa',\sigma')}{V_D}\left\{[1-p(\kappa,\kappa',d)] + p(\kappa,\kappa',d)x\int \phi(w|\kappa,\sigma,\kappa',\sigma',d)\mathrm{e}^{-wy}dw\right\}d\boldsymbol{x'}d\sigma' d\kappa'\right]^{N-1} \ . \tag{A5}$$

1. The degree of nodes

From Eq. (A5), we can readily see that the average degree of nodes with hidden variables κ and σ only depends on κ [43]

$$\bar{k}(\kappa,\sigma) = \left.\frac{\partial\hat{g}(x,y|\kappa,\sigma)}{\partial x}\right|_{x=1,y=0} = \frac{N-1}{V_D}\iiint \rho(\kappa',\sigma')p(\kappa,\kappa',d)d\boldsymbol{x'}d\sigma' d\kappa' = \delta\iint \rho(\kappa')p(\kappa,\kappa',d)d\boldsymbol{x'}d\kappa' \ , \tag{A6}$$

where $\rho(\kappa)$ is the marginal pdf of $\rho(\kappa,\sigma)$, and where $\delta \equiv N/V_D$ is the density of nodes in the metric space (we consider here that $N \gg 1$). Using the definition of $p(\kappa,\kappa',d)$ given in Sec. II and switching to D-dimensional spherical coordinates (Ω_D is the solid angle subtended by a D-dimensional object), this last equation becomes

$$\bar{k}(\kappa) = \delta \iiint \rho(\kappa')p(\chi)r^{D-1}drd\Omega_D d\kappa' = \frac{2\pi^{D/2}\delta\mu}{\Gamma(D/2)}\kappa \int \kappa'\rho(\kappa')d\kappa' \int \chi^{D-1}p(\chi)d\chi = \frac{2\pi^{D/2}\delta\mu\langle\kappa\rangle I_1}{\Gamma(D/2)}\kappa \ , \tag{A7}$$

where we have noted $\langle\kappa\rangle = \int \kappa\rho(\kappa)d\kappa$ and $I_1 = \int \chi^{D-1}p(\chi)d\chi$. The average degree for the whole network is

$$\langle k\rangle = \int \bar{k}(\kappa)\rho(\kappa)d\kappa = \frac{2\pi^{D/2}\delta\mu I_1}{\Gamma(D/2)}\langle\kappa\rangle^2 \ . \tag{A8}$$

Consequently, we see that the free parameter μ can be chosen such that $\bar{k}(\kappa) = \kappa$ and $\langle k\rangle = \langle\kappa\rangle$. The degree distribution of the networks generated by the model can therefore be controlled through the pdf $\rho(\kappa)$. Following similar steps, we also find that

$$\mathrm{Var}[k(\kappa)] = \bar{k}(\kappa) \ , \tag{A9}$$

which implies that

$$\frac{\sqrt{\mathrm{Var}[k(\kappa)]}}{\bar{k}(\kappa)} = \frac{1}{\sqrt{\kappa}} \ . \tag{A10}$$

In other words, nodes with a same high value of their hidden variable κ tend to all have a degree close to the expected value $\bar{k}(\kappa) = \kappa$.

2. The degree distribution

By definition, evaluating Eq. (A5) at $y = 0$ yields the generating function for the degree distribution of nodes with hidden variable κ

$$\hat{g}(x,0|\kappa,\sigma) \equiv \sum_k g(k|\kappa)x^k \ . \tag{A11}$$

Assuming $N \gg 1$ and using Eq. (A6), we obtain

$$\hat{g}(x,0|\kappa,\sigma) = \left[1 + (x-1)\frac{\bar{k}(\kappa)}{N-1}\right]^{N-1} = \exp\left\{(x-1)\bar{k}(\kappa)\right\} = \sum_k \frac{\mathrm{e}^{-\bar{k}(\kappa)}\bar{k}(\kappa)^k}{k!}x^k \ . \tag{A12}$$

In other words, the degrees of nodes with hidden variable κ follow a Poisson distribution with mean $\bar{k}(\kappa)$ [43]. Using $\bar{k}(\kappa) = \kappa$, the degree distribution of the whole network is therefore

$$P(k) = \int g(k|\kappa)\rho(\kappa)d\kappa = \frac{1}{k!}\int \mathrm{e}^{-\kappa}\kappa^k\rho(\kappa)d\kappa \ , \tag{A13}$$

thus unveiling the precise link between $\rho(\kappa)$ and $P(k)$.

3. The strength of nodes

Following similar steps as in Sec. A 1, we can compute the average strength of nodes with hidden variables κ and σ

$$\bar{s}(\kappa,\sigma) = -\left.\frac{\partial\hat{g}(x,y|\kappa,\sigma)}{\partial y}\right|_{x=1,y=0} = \delta \iiint \rho(\kappa',\sigma')p(\kappa,\kappa',d)\int w\phi(w|\sigma,\sigma',d)dwd\boldsymbol{x'}d\sigma'd\kappa'$$

$$= \frac{2\pi^{D/2}\delta\mu^{1-\alpha/D}\nu I_2}{\Gamma(D/2)}\sigma \int \sigma'\rho(\sigma')d\sigma' \int \chi^{D-\alpha-1}p(\chi)d\chi \frac{2\pi^{D/2}\delta\mu^{1-\alpha/D}\nu I_2\langle\sigma\rangle I_3}{\Gamma(D/2)}\sigma \ , \tag{A14}$$

where $\rho(\sigma)$ is the other marginal pdf of $\rho(\kappa,\sigma)$, and where we have noted $\langle\sigma\rangle = \int \sigma\rho(\sigma)d\sigma$, $I_2 = \int wf(w)dw$, and $I_3 = \int \chi^{D-\alpha-1}p(\chi)d\chi$. We therefore conclude that the strength of nodes only depends on σ, hence $\bar{s}(\kappa,\sigma) = \bar{s}(\sigma)$. The average strength for the whole network is

$$\langle s\rangle = \int \bar{s}(\sigma)\rho(\sigma)d\sigma = \frac{2\pi^{D/2}\delta\mu^{1-\alpha/D}\nu I_2 I_3}{\Gamma(D/2)}\langle\sigma\rangle^2 \ . \tag{A15}$$

As for the average degree, we see that we can set the free parameter ν such that $\bar{s}(\sigma) = \sigma$ and $\langle s\rangle = \langle\sigma\rangle$. The strength distribution of the networks generated by the model can therefore be controlled through the pdf $\rho(\sigma)$. Following similar steps, we find that

$$\mathrm{Var}[s(\kappa,\sigma)] = \delta \iiint \rho(\kappa',\sigma')p(\kappa,\kappa',d)\int w^2\phi(w|\sigma,\sigma',d)dwd\boldsymbol{x'}d\sigma'd\kappa' = \frac{2\pi^{D/2}\delta\mu^{1-2\alpha/D}\nu^2 I_4\langle\sigma^2/\kappa\rangle I_5}{\Gamma(D/2)}\frac{\sigma^2}{\kappa} \ , \tag{A16}$$

where we have noted $\langle\sigma^2/\kappa\rangle = \iint(\sigma^2/\kappa)\rho(\kappa,\sigma)d\sigma d\kappa$, $I_4 = \int w^2 f(w)dw$ and $I_5 = \int \chi^{D-2\alpha-1}p(\chi)d\chi$. Setting μ such that $\langle k\rangle = \langle\kappa\rangle$ [see Eq. (A8)], we find that

$$\frac{\sqrt{\mathrm{Var}[s(\kappa,\sigma)]}}{\bar{s}(\sigma)} = \frac{\sqrt{\bar{\kappa}\langle\sigma^2/\kappa\rangle I_1 I_4 I_5}}{\langle\sigma\rangle I_2 I_3}\frac{1}{\sqrt{\kappa}} \ , \tag{A17}$$

i.e., the strength of high-degree nodes is close to its expected value given by Eq. (A14).

4. The strength of nodes of degree k

Unfortunately, it is not possible to obtain a general closed form of the pdf $g(s|\kappa,\sigma)$, similar to Eq. (A12), from Eq. (A5). We can however characterize the strengths of nodes through the average strength of nodes with a given degree, $\bar{s}(k)$. Let us first explicit its calculation

$$\bar{s}(k) = \int sg(s|k)ds = \frac{1}{P(k)}\int sg(k,s)ds = \frac{1}{P(k)}\iint\left[\int sg(k,s|\kappa,\sigma)ds\right]\rho(\kappa,\sigma)d\sigma d\kappa \ . \tag{A18}$$

From Eq. (A4), we see that the integral in brackets can be obtained from Eq. (A5)

$$-\left.\frac{\hat{g}(x,y|\kappa,\sigma)}{\partial y}\right|_{y=0} = \sum_k\left[\int sg(k,s|\kappa,\sigma)ds\right]x^k \ . \tag{A19}$$

Assuming $N \gg 1$ and using Eqs. (A7) and (A14), we find

$$-\left.\frac{\hat{g}(x,y|\kappa,\sigma)}{\partial y}\right|_{y=0} = x\bar{s}(\sigma)\left[1+(x-1)\frac{\bar{k}(\kappa)}{N-1}\right]^{N-2} = x\bar{s}(\sigma)\exp\left\{(x-1)\bar{k}(\kappa)\right\} = \sum_{k>0}\left[\frac{\bar{s}(\sigma)\mathrm{e}^{-\bar{k}(\kappa)}\bar{k}(\kappa)^{k-1}}{(k-1)!}\right]x^k \ . \tag{A20}$$

Excluding the case $k = 0$ in this last expression is not problematic since $g(s|0) = \delta(s)$, by definition, and therefore the coefficient in front of x^0 must be zero [see Eq. (A19)]. Combining Eqs. (A18)–(A20), $\bar{k}(\kappa) = \kappa$ and $\bar{s}(\sigma) = \sigma$, we obtain

$$\bar{s}(k) = \frac{1}{(k-1)!P(k)}\iint\sigma\mathrm{e}^{-\kappa}\kappa^{k-1}\rho(\kappa,\sigma)d\sigma d\kappa \ , \tag{A21}$$

thus further clarifying how the joint pdf $\rho(\kappa,\sigma)$ controls the correlation between the degree and the strength of nodes. In fact, assuming no correlation, i.e., $\rho(\kappa,\sigma) = \rho(\kappa)\rho(\sigma)$, yields $\bar{s}(k) = \langle\sigma\rangle$, which is independent of the degree, as expected.

Appendix B: A practical test of the triangle inequality

To test the triangle inequality in a given weighted complex network, we first find the parameters μ, β, and γ that best match the empirical topology. To achieve the optimal matching, we first use the empiric sequence of degrees as input for the sequence of κ's so that the fluc-

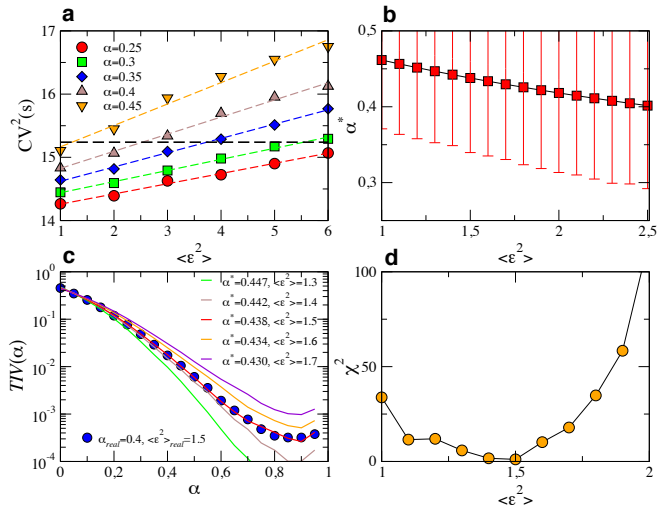

FIG. 9. Test of the triangle inequality applied to a synthetic network generated with $\alpha_{real} = 0.4$ and noise $\langle\epsilon^2\rangle = 1.5$. **a**, the square of the coefficient of variation of nodes' strength as a function of the noise $\langle\epsilon^2\rangle$ in synthetic weighted networks with different values of α. The horizontal dashed line is the empirical value measured in the input network. **b**, values of α^* as a function of the noise obtained from the intersection of the dashed line in **a** with the synthetic curves. **c**, $TIV(\alpha)$ curves for synthetic networks with the values of α^* and $\langle\epsilon^2\rangle$ from **b** compared to the same function for the input network. **d**, χ^2 statistics obtained from the comparison of function $TIV(\alpha)$ between the model and input network.

tuations in the tail of the degree distribution of the input network are preserved. Subsequently, the sequence of κ's is slightly modified to maximize the similarity between the degree distribution and clustering coefficient of synthetic networks and the real one. After this process, the sequence of κ's is kept fixed during the rest of the process.

The sequence is then used to generate different weighted networks as follows. From the empiric relation strength-degree, we measure the exponent η, as well as the first and second moments of the strength distribution $\langle s^2\rangle$ and $\langle s\rangle$. For fixed values of α and $\langle\epsilon^2\rangle$, we generate a large number of synthetic weighted networks and measure the average value of $CV^2(s)$ and its ensemble fluctuations. In Fig. 9**a**, we show $CV^2(s)$ as a function of $\langle\epsilon^2\rangle$ and different values of α for one of the synthetic networks used in Fig. 4 with $\alpha_{real} = 0.4$ and noise $\langle\epsilon^2\rangle = 1.5$. The intersection of these curves with the empirical value of $CV^2(s)$ defines a collection of α's as a function of the noise, $\alpha^*\left(\langle\epsilon^2\rangle\right)$, which become the potential candidates to be the estimate of α_{real}, see Fig. 9**b**. Finally, for each pair $(\langle\epsilon^2\rangle, \alpha^*)$ in Fig. 9**b** we measure the function $TIV(\alpha)$ and compare it with the same function measured in the input network, see Fig. 9**c**. The comparison is performed by measuring the standard χ^2 statistics. The inferred value of α_{real} corresponds to the value of $\alpha^*(\langle\epsilon^2\rangle)$ minimizing the value of χ^2, see Fig. 9**d**. To find a lower bound of the inferred value of α_{real}, we use the ensemble fluctuations of $CV^2(s)$. For any fixed value of $\langle\epsilon^2\rangle$, the lower bound of α^* is the value of α that is still able to reproduce the empirical value of $CV^2(s)$ (see Fig. 9**b**). The lower bound for the inferred value of α_{real} is the lower bound of α^* that corresponds to the optimal value of the noise $\langle\epsilon^2\rangle$ in Fig. 9**d**.

[1] Mark Newman, *Networks: An Introduction* (Oxford University Press, Inc., New York, NY, USA, 2010).

[2] R. Cohen and S. Havlin, *Complex Networks: Structure, Robustness and Function* (Cambridge University Press, 2010).

[3] M. Á. Serrano, D. Krioukov, and M. Boguñá, "Self-similarity of complex networks and hidden metric spaces," Phys. Rev. Lett. **100**, 078701 (2008).

[4] M. Boguñá and D. Krioukov, "Navigating ultrasmall worlds in ultrashort time," Phys. Rev. Lett. **102**, 058701 (2009).

[5] M. Boguñá, D. Krioukov, and K. C. Claffy, "Navigability of complex networks," Nat. Phys. **5**, 74–80 (2009).

[6] D. Krioukov, F. Papadopoulos, M. Kitsak, A. Vahdat, and M. Boguñá, "Hyperbolic geometry of complex networks," Phys. Rev. E **82**, 036106 (2010).

[7] L. Gugelmann, K. Panagiotou, and U. Peter, "Random hyperbolic graphs: Degree sequence and clustering," in *Automata, Languages, and Programming*, Lecture Notes in Computer Science, Vol. 7392, edited by Artur Czumaj, Kurt Mehlhorn, Andrew Pitts, and Roger Wattenhofer (Springer Berlin Heidelberg, 2012) pp. 573–585.

[8] M. Bode, N. Fountoulakis, and T. Müller, "On the giant component of random hyperbolic graphs," in *The Seventh European Conference on Combinatorics, Graph Theory and Applications*, CRM Series, Vol. 16, edited by Jaroslav Nešetřil and Marco Pellegrini (Scuola Normale Superiore, 2013) pp. 425–429.

[9] E. Candellero and N. Fountoulakis, "Clustering and the hyperbolic geometry of complex networks," in *Algorithms and Models for the Web Graph*, Lecture Notes in Computer Science, Vol. 8882, edited by Anthony Bonato, Fan Chung Graham, and Paweł Pralat (Springer International Publishing, 2014) pp. 1–12.

[10] T. Friedrich and A. Krohmer, "On the diameter of hyperbolic random graphs," in *Automata, Languages, and Programming*, Lecture Notes in Computer Science, Vol. 9135, edited by Magnús M. Halldórsson, Kazuo Iwama, Naoki Kobayashi, and Bettina Speckmann (Springer Berlin Heidelberg, 2015) pp. 614–625.

[11] F. Papadopoulos, M. Kitsak, M. Á. Serrano, M. Boguñá, and D. Krioukov, "Popularity versus similarity in growing networks," Nature **489**, 537–540 (2012).

[12] A. Gulyás, J. J. Bíró, A. Kőrösi, G. Rétvári, and D. Krioukov, "Navigable networks as Nash equilibria of navigation games," Nat. Commun. **6**, 7651 (2015).

[13] M. Boguñá, F Papadopoulos, and D. Krioukov, "Sustaining the Internet with hyperbolic mapping," Nat.

Commun. **1**, 62 (2010).
[14] M. Á. Serrano, M. Boguñá, and F. Sagués, "Uncovering the hidden geometry behind metabolic networks," Mol. Biosyst. **8**, 843–850 (2012).
[15] A. Barrat, M. Barthélemy, R. Pastor-Satorras, and A. Vespignani, "The architecture of complex weighted networks." Proc. Natl. Acad. Sci. U. S. A. **101**, 3747–52 (2004).
[16] M. A. Serrano, "Rich-club vs rich-multipolarization phenomena in weighted networks," Phys. Rev. E **78**, 026101 (2008).
[17] D. Brockmann and D. Helbing, "The Hidden Geometry of Complex, Network-Driven Contagion Phenomena," Science **342**, 1337–1342 (2013).
[18] G. Bianconi, "Emergence of weight-topology correlations in complex scale-free networks," Europhys. Lett. **71**, 1029–1035 (2004).
[19] A. Barrat, M. Barthélemy, and A. Vespignani, "Weighted Evolving Networks: Coupling Topology and Weight Dynamics," Phys. Rev. Lett. **92**, 228701 (2004).
[20] S. Yook, H. Jeong, A.-L. Barabási, and Y. Tu, "Weighted Evolving Networks," Phys. Rev. Lett. **86**, 5835–5838 (2001).
[21] J. M. Kumpula, J.-P. Onnela, J. Saramäki, K. Kaski, and J. Kertész, "Emergence of Communities in Weighted Networks," Phys. Rev. Lett. **99**, 228701 (2007).
[22] T. Antal and P. L. Krapivsy, "Weight-driven growing networks," Phys. Rev. E **71**, 026103 (2005).
[23] D. Zheng, S. Trimper, B. Zheng, and P. M. Hui, "Weighted Scale-Free Networks with Stochastic Weight Assignments," Phys. Rev. E **67**, 040102(R) (2003).
[24] W.-X. Wang, B. Hu, T. Zhou, B.-H. Wang, and Y.-B. Xie, "Mutual selection model for weighted networks," Phys. Rev. E **72**, 046140 (2005).
[25] M. Li, D. Wang, Y. Fan, Z. Di, and J. Wu, "Modelling weighted networks using connection count," New J. Phys. **8**, 72 (2006).
[26] R. Mastrandrea, T. Squartini, G. Fagiolo, and D. Garlaschelli, "Enhanced reconstruction of weighted networks from strengths and degrees," New J. Phys. **16**, 043022 (2014).
[27] D. Garlaschelli, "The weighted random graph model," New J. Phys. **11**, 073005 (2009).
[28] D. Garlaschelli and M. Loffredo, "Generalized Bose-Fermi Statistics and Structural Correlations in Weighted Networks," Phys. Rev. Lett. **102**, 038701 (2009).
[29] O. Sagarra, C. Pérez Vicente, and A. Díaz-Guilera, "Statistical mechanics of multiedge networks," Phys. Rev. E **88**, 062806 (2013).
[30] O. Sagarra, C. J. Pérez Vicente, and A. Díaz-Guilera, "Role of adjacency-matrix degeneracy in maximum-entropy-weighted network models," Phys. Rev. E **92**, 052816 (2015).
[31] M. Barthélemy, A. Barrat, R. Pastor-Satorras, and A. Vespignani, "Characterization and modeling of weighted networks," Physica A **346**, 34–43 (2005).
[32] We take D-dimensional spheres of radius R. However, the constraint of having constant density implies that the radius diverges in the thermodynamic limit and, thus, the metric space is equivalent to a D-dimensional Euclidean space.
[33] It is common to set $\kappa_c = \kappa_0 N^{1/(\gamma-1)}$, i.e., the *natural* cut-off of a scale-free distribution [44, 45]. However, in general κ_c can take any value in response to particular mechanisms at play, like the limited capacity to handle more than a given number of connections in the airport network.
[34] The generalized incomplete gamma function is defined as $\Gamma(t, z_0, z_1) = \int_{z_0}^{z_1} z^{t-1}\mathrm{e}^{-z}dz$ (the regular complete and incomplete gamma functions can be retrieved by setting the bounds z_0 and z_1 to the appropriate values). Whenever $1 \sim z_0 \ll z_1$, a condition holding for most realistic degree distributions, the double incomplete gamma function scales as $\Gamma(n+\epsilon, \kappa_0, \kappa_c) \sim \Gamma(n)n^{\epsilon}$ with $n \in \mathbb{N}$ and $\epsilon \in \mathbb{R}$ [46].
[35] M. Á. Serrano, M. Boguñá, and R. Pastor-Satorras, "Correlations in weighted networks," Phys. Rev. E **74**, 055101 (2006).
[36] Also note that parameter ν also depends on α.
[37] J. D. Orth *et al.*, "A comprehensive genome-scale reconstruction of *Escherichia coli* metabolism - 2011," Mol. Syst. Biol. **7**, 535 (2011).
[38] Data freely available at the website of the U.S. Bureau of Transportation Statistics (`transtats.bts.gov`, table T-100).
[39] M. Á Serrano and M. Boguñá, "Topology of the world trade web," Phys Rev E **68**, 015101 (2003).
[40] M. Á. Serrano, M. Boguñá, and A. Vespignani, "Extracting the multiscale backbone of complex weighted networks," Proc. Natl. Acad. Sci. USA **106**, 6483–6488 (2009).
[41] G. García-Pérez, M. Boguñá, A. Allard, and M. Á. Serrano, "Rethinking distance in international trade: World Trade Atlas 1870-2013," arXiv:1512.02233 (2015).
[42] D. Krioukov, F. Papadopoulos, A. Vahdat, and M. Boguñá, "Curvature and temperature of complex networks," Phys. Rev. E **80**, 035101 (2009).
[43] M. Boguñá and R. Pastor-Satorras, "Class of correlated random networks with hidden variables," Phys. Rev. E **68**, 036112 (2003).
[44] S. N. Dorogovtsev and J. F. F. Mendes, "Evolution of networks," Adv. Phys. **51**, 1079–1187 (2002).
[45] M. Boguñá, R. Pastor-Satorras, and A. Vespignani, "Cut-offs and finite size effects in scale-free networks," Eur. Phys. J. B **38**, 205–209 (2004).
[46] F. W. J. Olver, D. W. Lozier, R. F. Boisvert, and C. W. Clark, *NIST Handbook of Mathematical Functions* (Cambridge University Press, New York, NY, 2010).